A Distributed Beamforming Scheme for LEO Satellite Direct Connectivity with Satellite Selections and Phase Adjustment

Qianyi Ouyang, Zhishu Qu, *Member, IEEE,* and Yue Gao, *Fellow, IEEE*

***Abstract*—Among LEO satellites communications, direct connectivity to user equipment (UE) has drawn much attention for its ability of providing basic emergent services. However, the link budget shortage resulting from long propagation length limits the capacity of communications. Distributed beamforming is a solution that provides high power gain by utilizing multiple transmitters simultaneously. Thus, this work presents a distributed beamforming scheme for LEO satellites direct connectivity services that can provide high power gain for multiple ground UEs regardless of their locations. By selecting satellites from a set of available ones and optimizing the transmit phases of electromagnetic waves on satellites, all the ground UEs can receive power gains improvement. Also, this work considers satellite motions by proposing a fast algorithm that adjusts phases according to changing satellite locations. Finally, a satellite re-selection process is designed to ensure constant power gain as satellites become unavailable. Simulation results demonstrate the effectiveness of our design, with up to 7dB of power gain improvement for static satellites and around 3dB for moving satellites.**

***Index Terms*—LEO satellites, direct connectivity, distributed beamforming, UE, power gain improvement.**

I. INTRODUCTION

Satellite communication networks include Geosynchronous Earth Orbit (GEO) satellites, Medium Earth Orbit (MEO) satellites, and Low Earth Orbit(LEO) satellites. Among them, LEO satellites have drawn much attention due to the large satellite constellations. For example, OneWeb has 720 satellites, SpaceX has 4425 satellites and Telesat has 117 satellites [1]. Networks can be formed among satellites and this leads to the ability to provide global broadband access. LEO satellite architecture brings a revolution to traditional communications by offering promising service continuity, wide-area coverage, and availability for critical and emergent situations [2]. Also, several factors benefit the development of LEO satellites, including better launching and rocket reuse technologies, developed digital signal processing techniques, and advanced antenna design [3].

Among all types of satellite communications, direct communications with User Equipment (UE) have raised much attention in recent years. This includes satellite-to-device, satellite-to-handset and satellite-to-phone. This direct connectivity can provide basic services in emergencies, thus researchers and companies are paying much attention to developing their own solutions [4]-[7]. However, the poor link budget is a major problem with the direct connectivity to UE. The link budgets for three LEO constellations are presented in [1]. The long propagation path leads to severe signal attenuation. Also, increasing signal frequency for wider bandwidth increases attenuation, making the link budget even poorer.

Several solutions to this issue have been presented. Lynk successfully establishes communications between satellites and cellular UE, however, only the message service is available due to the limited bandwidth [7]. Besides, satellite Multiple-Input Multiple-Output (MIMO) has been considered as a solution. [8]-[12] study satellite MIMO communications from different perspectives. A massive MIMO transmission scheme is presented in [8]. They conduct frequency reuse and analyze the statistical channel state information to avoid channel estimation. [11] study the downlink transmission for MIMO by considering a slow-varying channel at the transmitter. A learning-based on-board precoding optimization is designed and solved. [12] take service fairness into consideration and develop a downlink MIMO scheme that divides user terminals into groups. Although focusing on various aspects, the common problem with the MIMO approach is that the receiver power gain is still limited. Suppose that there are M transceivers, the maximum gain at the receiver is M, which is still inadequate for direct connectivity applications.

Another solution is distributed beamforming, which can ideally achieve M^2 power gain [13]. A few research studies the applications of distributed beamforming. In [14], a distributed beamforming approach addressing the energy efficiency problem is proposed. The feasibility in conditions of imperfect

This work is supported by the China Postdoctral Science Foundation under Grant 2023TQ0076. (Corresponding author: Zhishu Qu)

Qianyi Ouyang, Zhishu Qu and Yue Gao are with the School of Computer Science, Fudan University, Shanghai 200437, China (e-mail: zhishu_qu@fudan.edu.cn).

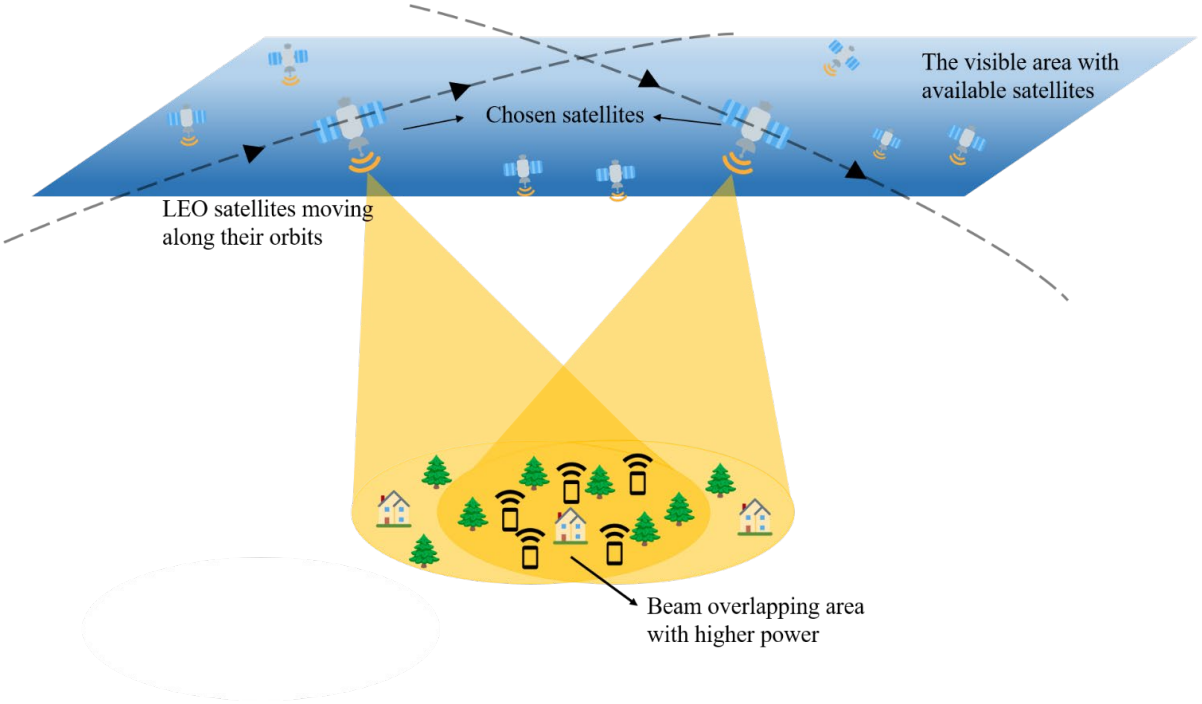

Fig. 1. An illustration of satellite distributed beamforming.

signal synchronization is examined. [15]-[17] study the synchronization problem of distributed beamforming. [15] realize signal synchronization by applying wireless phase and frequency synchronization. In [18], the quality-of-service and security is considered in a wireless distributed beamforming network. [19] design a joint distributed beamforming optimization problem which considers beam pattern, transmission power and energy consumption. These works, although applying distributed beamforming, do not focus on utilizing the power gain advantages. [20]-[25] study distributed beamforming in unmanned vehicle applications, in which distributed unmanned vehicles serve as transmitters. The flexibility of unmanned vehicles is an advantage of such systems. However, since the channel condition and propagation distance differ from LEO satellite scenarios, these applications cannot be utilized in LEO satellites scenarios directly. [26]-[29] apply distributed beamforming in wireless power transfer. They study the power gain condition of the UE area and utilize the power gain of distributed beamforming. Although no information is contained during power transmission, the study of the principle of power gain improvement is inspiring.

Among research on distributed beamforming, [30] propose a distributed beamforming scheme for LEO satellites, where the overlapping area of the beams of several satellites is utilized. By studying the interfering phenomenon of electromagnetic (EM) waves, it is found that in certain locations there is a M^2 fold power gain for M satellites. This is fundamental for improving the link budget of direct connectivity. The problem with this work is that it does not consider the location of UEs. If UE is located in the region where EM waves destructively interfere, the power gain is unacceptable. Besides, the satellite motion, which seriously affects the power gain condition on the ground, is not considered.

This work presents an LEO satellite distributed beamforming scheme that ensures ideal power gain regardless of UE locations and number. By selecting satellites from all available satellites and adjusting the transmit phase of EM waves on satellites, all ground UEs can achieve ideal power gain. Furthermore, the satellites' motions are considered. An algorithm is designed to ensure consistent sufficient power gain for ground users as satellites move. Finally, a satellite reselection process is proposed to make sure UEs receive ideal power gain when satellites are no longer available.

The contributions of this work can be summarized as follows:

- This work analyzes how satellite locations and phases of transmit EM waves influence the interference of EM waves. The interference is shown by a figure of power gain distribution and its formation and variations are studied.
- A distributed beamforming algorithm for multiple ground UEs is presented. By selecting appropriate satellites and calculating transmit phases, all UEs can receive ideal power gain, no matter where UEs are located.
- This work considers the satellite motion. A fast algorithm that update transmit phases according to the motion of satellites is proposed. UEs can receive constant ideal power gain as satellites move.
- A satellite re-selection process is designed to provide sustainable power gain improvement for UEs when satellites move out of the available range.

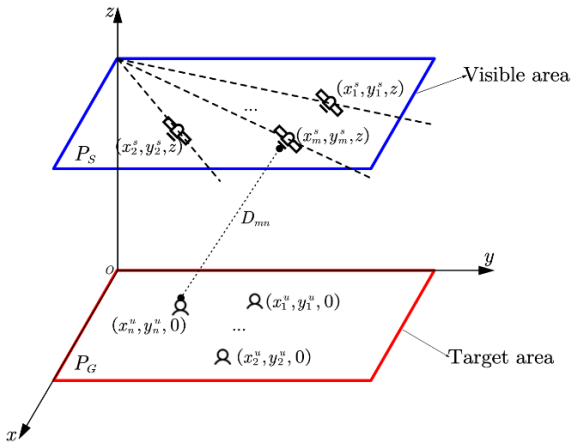

Fig. 2. The mathematical system model.

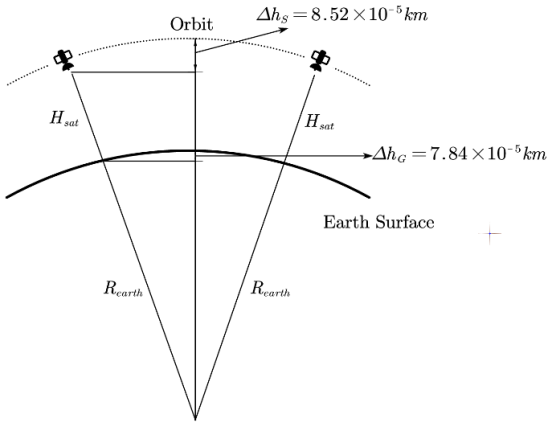

Fig. 3. The original model.

II. System Model and Problem Formulation

A. System Model

The illustration of the satellite distributed beamforming scenario is illustrated in Fig. 1. The overlapped region of multiple satellites is utilized to provide service for randomly distributed UEs on the ground. This shared area receives high power gains, thus the communication link budget for the users is enhanced.

Fig. 2 is the system mathematical model, where N ground users are randomly distributed in the P_G plane, within the target area where beams overlap. M satellites are available to be chosen from a set of M_a available satellites all in the P_S plane. Each satellite has a track and is considered available to be selected within the available area. Once they are selected, they become unavailable only after a short available time and satellites will be re-selected. This will be discussed in section IV. The distance D_{mn} is the distance between satellite m and user n.

Note that our system model is a simplified model of the real satellite orbit and earth surface. The real-world model is shown in Fig. 3, Δh_S and Δh_G are calculated according to the parameters in Table I. They are small enough to be ignored, thus the two arc faces (the earth's surface and the satellite orbit) can be simplified as planes.

B. Changing the Power Distribution

It is analyzed in [30] that when the beam coverage of multiple satellites overlaps, the transmitting EM waves constructively interfere with each other. Considering the power gain distribution on the ground, the interference leads to fringes of spot beams in terms of satellite number. Fig. 4 is an example of this distribution. (a), (b) are the cases with 2 satellites and (c), (d) with 4 satellites.(b) and (d) are the vertical view figures of (a) and (c), respectively. It can be seen that 2 satellites form fringes and 4 satellites form spots. The former achieve 6dB power gain and the latter 12dB. This corresponds to the mentioned M^2 fold power gain.

The principle behind this phenomenon is that the propagation path between different satellites and locations on the ground varies, causing different EM wave phase delays. When the phases are aligned, the highest power gains are achieved, while when waves are out of phase, they form the lowest power gain. This resembles the physical phenomenon of the famous double-slit experiment (when there are 2 satellites). The wave path difference forms fringes or spot beams.

The phase delay caused by the propagation route can be denoted as:

$$\varphi_{mn}^{p} = 2\pi \frac{D_{mn}}{\lambda}, \tag{1}$$

where D_{mn} is the distance between a satellite m and a ground user n. λ denotes the wavelength of the transmitting EM wave.

For simplicity, we only consider the E-field. The E-wave transmitted by satellite m can be derived as:

$$E_m = A_m \exp[j(2\pi f_{EM} t + \varphi_m^s)] \tag{2}$$

where A is the amplitude and φ_m^s is the initial phase of the wave transmitted by the satellite.

Thus the E-wave arriving at ground node n becomes:

$$E_{mn} = A_m \exp[j(2\pi f_{EM} t + \varphi_{mn}^{p} + \varphi_m^s)] \tag{3}$$

The polarization method can affect the superposition of EM-wave from different satellites. In [30], linear polarization is analyzed and proves that the difference of polarization directions can lead to a gain loss when the satellites are not moving in parallel tracks. In this article, we consider circular polarization instead of linear polarization for two reasons: Firstly, it is more common in satellite communications. Secondly, even when satellite tracks intersect with each other, circular polarization does not necessarily lead to a power gain loss. The illustration is shown in Fig. 5. θ is the track angle and Θ is the rotation angle of circularly polarized EM waves transmitted by the satellites. When

$$\Theta_1 + \theta_1 = \Theta_2 + \theta_2 \tag{4}$$

The waves of two satellites are considered aligned. This means the effect of satellite track angles can be compensated by phase adjustment.

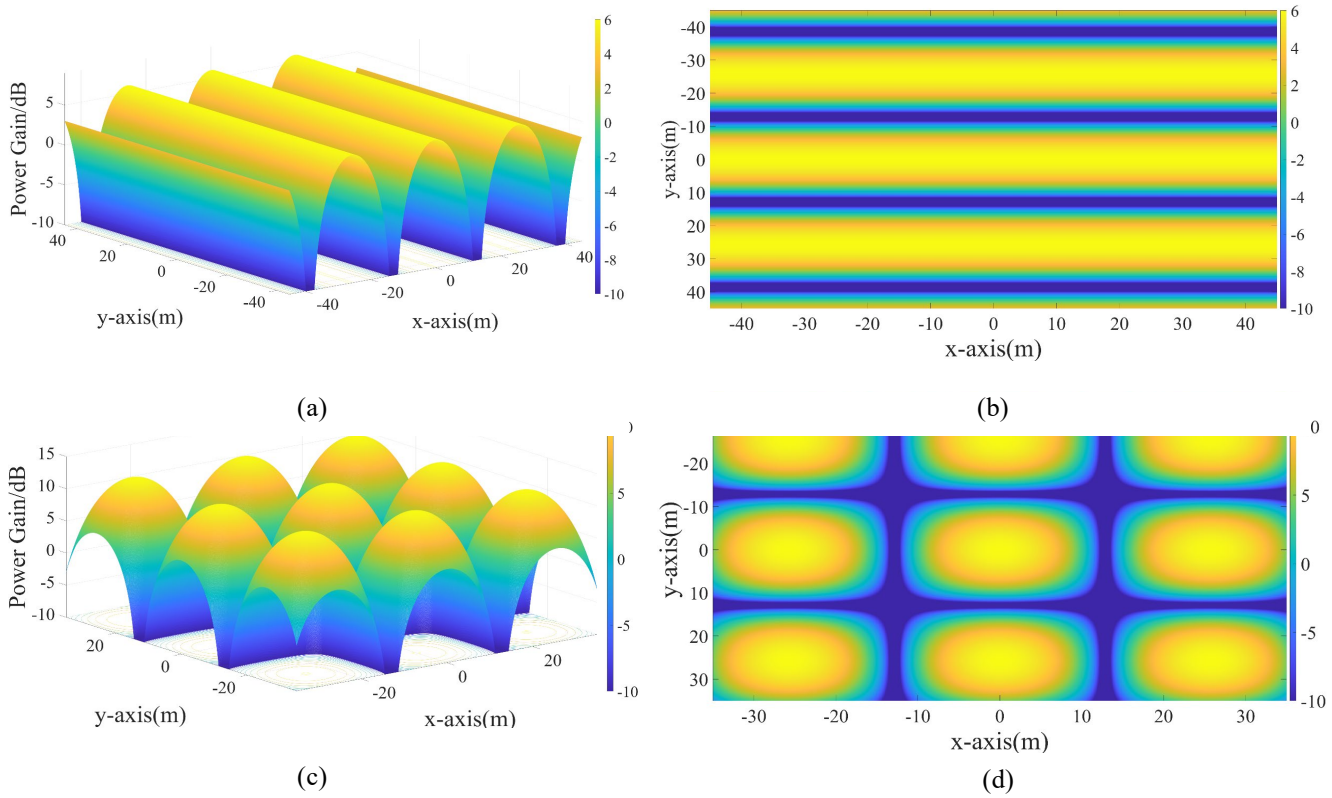

Fig. 4. Power gain distribution with fringes and spots.

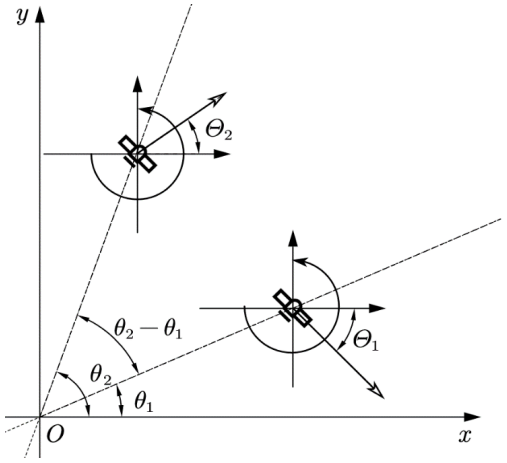

Fig. 5. The relationship between circular polarization and satellite tracks.

By including the track angle effect in the adjustment of φ^s, the superposition signal of E-waves from all satellites for node n can be denoted as:

$$E_n = \sum_{m=1}^{M} A_m \exp[j(2\pi f_{EM} t + \varphi_{mn}^p + \varphi_m^s)] \tag{5}$$

The power of the signal can be calculated as:

$$P_n = \frac{1}{T}\int_0^T |E_n|^2 dt \tag{6}$$

The maximum power gain M^2 is achieved when all waves are constructively added, where the phase components satisfy:

$$\varphi_{an}^p + \varphi_a^s - \varphi_{bn}^p - \varphi_b^s = 2k\pi, k \in \mathrm{Z}, \forall a, b \in [1, M] \tag{7}$$

Substituting (1), (7) becomes:

$$2\pi \frac{D_{an} - D_{bn}}{\lambda} + \varphi_a^s - \varphi_b^s = 2k\pi, k \in \mathrm{Z}, \forall a, b \in [1, M] \tag{8}$$

According to (8), the power gain distribution varies as the path length D_{mn} and the initial phase φ_m^s changes. In other words, there is a certain ground power gain figure for a set of φ_m^s and D_{mn}. In the next section, the way of utilizing this power gain distribution is discussed.

III. Multiple UEs Distributed Beamforming

As shown in Fig. 4, along with the bright region of the highest power gain, there are dark regions where waves destructively interfere and have the lowest gain. When the serving UE is located in the dark area, the link budget is severely interrupted. The dark region of power gain on the ground is unavoidable due to the physical principle of EM-wave. However, we still want to utilize this periodic distribution to serve multiple UEs. In brief, to cover each UE with a beam of the highest power gain.

To achieve this, the power distribution should be controlled to force the bright region to cover the UEs, by adjusting the wave path D_{mn} and initial phase φ_m^s. The initial transmit phase is controlled with phased arrays on satellites. The transmit wave phase can be controlled by conducting the same phase shift to every array element. On the other hand, D_{mn} can be modified

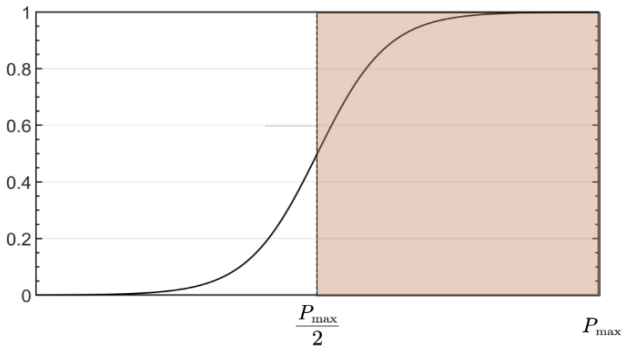

Fig. 2. The graph of *f(x)*.

by selecting satellites.To provide the ground users with the overall highest power gain, the most suitable satellites and their according transmit wave phases need to be optimized.

Suppose each satellite is equipped with a phased array of Q elements. Rewrite(2), the array synthesized signal on satellite m can be derived as:

$$E_m = \sum_{q=1}^{Q} A_q \exp[j(2\pi f_{EM} t + \varphi_m^s + \varphi_q^\phi)] \tag{9}$$

where A_q and φ_q^ϕ are the element gain and phase shift, respectively. The latter only controls the beam-pointing direction and is settled during our distributed beamforming process. A_q is also settled to be the largest available gain because it does not affect the distribution of ground power gain. Only φ_m^s is optimized. We define a set of available satellites S, each having its pre-settled track, and select M satellites. Locations of the chosen satellites are used to calculate the propagation route between satellite and ground nodes.(3) therefore becomes:

$$E_{mn} = \sum_{q=1}^{P} A_q \exp[j(2\pi f_{EM} t + \varphi_{mn}^p + \varphi_m^s + \varphi_q^\phi)] \tag{10}$$

The normalized average power is defined as:

$$p_{power}^{nor} = \sum_{n=1}^{N} \frac{P_n}{N P_{\max}} \tag{11}$$

where $P_{\max} = \left| \sum_{m=1}^{M} \sum_{q=1}^{Q} \left| A_q \right| \right|^2$, and $P_n = (\sum_{m=1}^{M} E_{mn})(\sum_{m=1}^{M} E_{mn}^*)$

However only optimizing the average power gain may lead to the imbalance of different UE. So a second function is added to ensure all UEs receive similar power gain improvement. It is a normalized variation limitation, which is defined as:

$$p_{thre}^{nor} = \sum_{n=1}^{N} \frac{f(P_n)}{N} \tag{12}$$

where function f is defined as:

$$f(x) = sigmoid(x - \frac{P_{\max}}{2}) = [1 + \exp(-x + \frac{P_{\max}}{2})]^{-1} \tag{13}$$

Fig. 6 shows the distribution of $f(x)$, as P_n approaches $P_{\max}$, the value approaches the maximum 1.

Combing these two functions, a weighted objective function

Algorithm 1 Genetic Algorithm-based Distributed Beamforming

Input: $S_{sat}, \mu, N_{MG}, p_{sel}, p_{mut}, N_{PS}, B_{sat}$
Output: J_{sat}, φ_{sat}

```
n = 1
Generate the 1th generation with N_ps M+1-dimension chromosomes
for n = 1 to N_MG do
    Use J_sat, extract the coordinates of selected satellites from B_sat.
    Fitness: Calculate the fitness function g of the individuals
    Select: Select the top p_sel best individuals to generate the next generation
    Crossover: Choose parents using the roulette wheel selection technique and exchange part of their chromosomes.
    Mutation: Flip the genes of individuals under p_mut
    Choose the individual u_best^n with the largest g
end for
Extract J_sat, φ_sat from u_best^{N_MG}
```

is thus defined as:

$$g(L_{sat}^{1\times M}, \varphi_m^{s\,1\times M}) = -\mu p_{thre}^{nor} - (1-\mu) p_{power}^{nor} \tag{14}$$

where $L_{sat}^{1\times M}$ is the locations of M satellites, which is chosen from a set of available satellites S_{sat}, $\varphi_m^{s\,1\times M}$ is the according satellite transmit phase, and μ is a weight factor. The first term is the average power gain, which is the mean of power gains at the locations of all nodes. The second term is a fairness term, which ensures all nodes receive similar power gains. g is set to be negative for minimization. This function is defined as the overall score of the power condition of the ground UE area.

The complete problem is formulated as follows:

$$\min_{L,\varphi} g \tag{15}$$

s.t
$$L \supset S_{sat} \tag{16}$$

$$\varphi \in [-\pi, \pi] \tag{17}$$

We choose Genetic Algorithm (GA) to solve the problem for the following reasons:

(1) The phase varies rapidly in a periodical manner as the satellite and node location changes, which leads to many equivalent solutions. GA searches for a global solution and can quickly get one of these equivalent solutions. Also it contains a mutation process which avoid local solutions.
(2) The satellite location is chosen from a set of available locations, making the function discrete. A search algorithm avoids calculating gratitude, which is better for this problem.
(3) The solution space has a low dimension. GA algorithm becomes easy to design and can converge quickly.

In GA, the values of phases of satellites are directly optimized. However, the selection of satellites need to be transferred to optimization of a value. Suppose S_{sat} contains N_S elements, thus there are $C_{N_S}^M$ ways of satellite selection. These

Algorithm 2 Distributed Beamforming on Time Slot n

Input: $\tilde{\varphi}_{n-1}, \alpha, \beta, \Delta$
Output: $\tilde{\varphi}_n$

Initialize: $x_0 = \tilde{\varphi}_{n-1}, i = 0$
repeat
  Calculate s
  if $\tilde{g}(x_i + s) < \tilde{g}(x_i)$ **then**
    $x_i = x_i + s$
  else
    $\Delta = \Delta(1 - \beta)$
  end if
  $i = i + 1$
until $||x_i - x_{i-1}|| < \alpha$
$\tilde{\varphi}_n = x_i$

selections are labeled, each representing a scheme of satellite choice. All the selections (transferred into satellite coordinates) form a matrix B_{sat}, with a size of $C_{N_s}^{M} \times M$. We optimize the selection scheme label J_{sat} to get the best satellite selection scheme.

Some predefined parameters of GA include: the max generations N_{MG}, the selection rate p_{sel}, the mutation rate p_{mut}, and the population size N_{PS}.The process of GA is shown in Algorithm I. The satellite location is transferred to a single value, thus an *M+1*-dimension solution is achieved after optimization. The satellite selection scheme and the according transmit on each satellite are thus extracted.

IV. The Satellite Motion

A. Phase Update

Algorithm I gets the best satellites and the according phases of the satellites. However, the satellites are moving, thus the calculated phases may be unsuitable for future satellite locations. This means UEs can only receive ideal power gain temporarily. An algorithm that can adaptively update the phases on satellites according to their motion is required to provide constant services for ground nodes.

Since the track is known and the satellite is moving at a constant speed, we assume that the location of satellite *m* at the *nth* time slot can be calculated as:

$$\tilde{L}(n) = (x_m^s(0), y_m^s(0), z) + v_{sat}(n-1)T(\cos\theta, \sin\theta, 0) \tag{18}$$

where $(x_m^s(0), y_m^s(0), z)$ is the initial satellite location, T is the update interval, θ is the track angle, and v_{sat} is the satellite velocity. Because these parameters are predefined, no extra time is needed to calculate satellite locations, which is important to our algorithm design.

The weight function also becomes time-varying, denoted as:

$$\tilde{g}(\tilde{L}_{sat}^{1\times M}(n), \varphi_m^{s\,1\times M}(n)) = \mu \tilde{p}_{pro}^{nor}(n) + (1-\mu)\tilde{p}_{power}^{nor}(n) \tag{19}$$

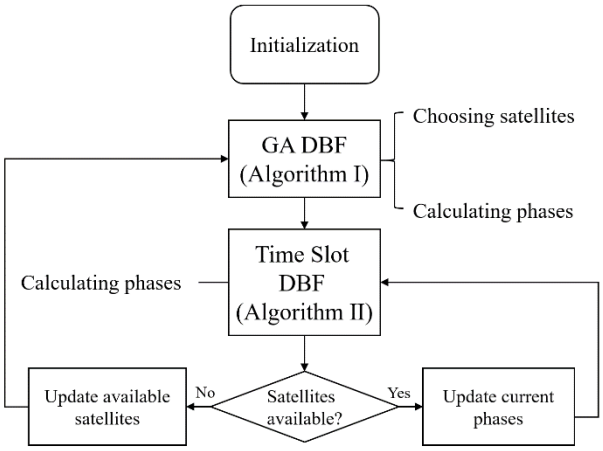

Fig. 3 Algorithm flowchart.

The problem is to solve $\varphi_m^{s\,1\times M}(n)$ at each time slot with the known satellite locations $\tilde{L}_{sat}^{1\times M}(n)$. The proposed GA-based algorithm is no longer useful due to its long calculation time. In detail, after the calculation, satellites move to other positions and the calculated phases are not suitable for new satellite locations. A new fast algorithm for moving satellites is necessary. Our idea is to recalculate the phases in each time slot according to the known satellite locations. The calculation time and update interval have to be short enough to make the phase constantly suitable for ground nodes.

Therefore, the new problem for time slot *n* becomes:

$$\min_{\tilde{\varphi}(n)} \tilde{g}(n) \tag{20}$$

s.t
$$\tilde{\varphi} \in [-\pi, \pi] \tag{21}$$

The solution space has an even lower dimension (M phases only), which saves calculation time. Also, (21) is a normalization of the phase, which can be conducted before or after solving the optimization problem. Thus this optimization can be considered unconstrained.

To get the solution, we introduce a unconstrained minimization method based on trust region and Quasi-Newton method. The advantages include:

a) An approximation of the objective function helps accelerate the calculation.
b) The phase of the former time slot can be utilized.

The process is as follows:

Define *G* as the trust region for $\tilde{g}(x)$ and *s* as the trial step. We search for a better solution that gets a smaller $\tilde{g}$ within *G*, i.e.

$$\tilde{g}(x+s) < \tilde{g}(x), x+s \in G \tag{22}$$

Define a quadratic approximation of $\tilde{g}$ as:

$$q(s) = \frac{1}{2}s^T Hs + s^T \nabla \tilde{g}(x) \tag{23}$$

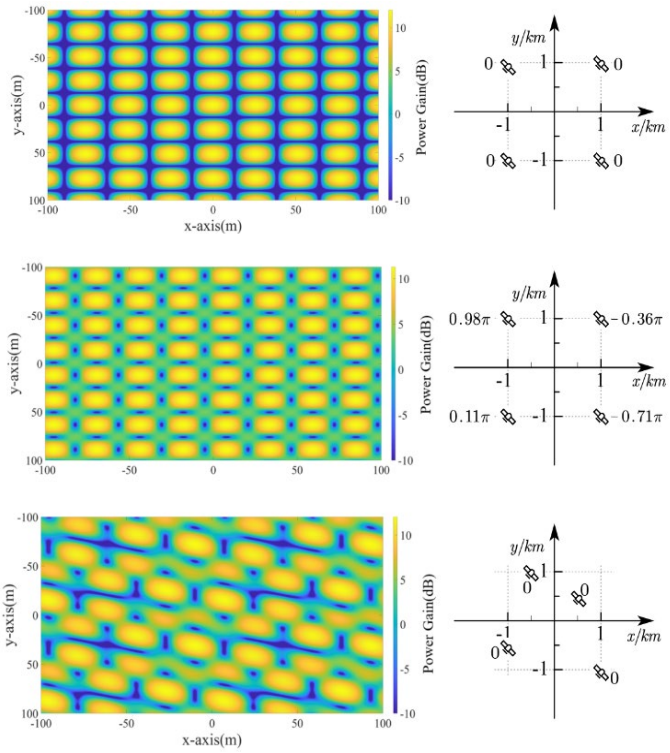

Fig. 8. Factors influencing ground power distribution.

which is the second-order Taylor approximation of $\tilde{g}$ at point x. H is the Hessian matrix.

The problem becomes:

$$\min_{s} q \tag{24}$$

$$\text{s.t} \quad \|Ds\| \le \Delta \tag{25}$$

where D is a diagonal scaling matrix and Δ is a positive scalar. A quick solution. A quick solution of this problem is achieved by considering a 2-dimension subspace, spanned by s_1 and s_2 [34], which satisfies:

$$s_1 = \nabla \tilde{g}(x) \tag{26}$$

$$H \cdot s_2 = -\nabla \tilde{g}(x) \tag{27}$$

The solution is given by:

$$\frac{1}{\Delta} - \frac{1}{\|s\|} = 0 \tag{28}$$

By iteratively update x and Δ, the solution of (20) is achieved. The process is shown in Algorithm II. Note that the initial point of each time slot is set to be the phases of the former time slot. This approach accelerates the search process.

Algorithm II is repeated as satellites move. By setting a short update interval T, this quick algorithm can get phases that are always suitable for changing satellite locations, providing consistent services for ground nodes.

B. Satellite Re-selection

Recall that satellites are selected from a set of available satellites and are only available in a finite period of time. In that

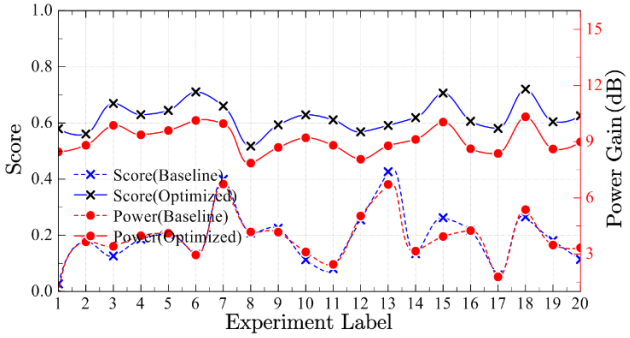

Fig. 9. Results of 20 experiment.

case, M satellites have to be re-chosen from a new set of available satellites and the related phases on satellites have to recalculated according to the algorithm presented in *C*. This leads to a loop, which is shown in Fig.7 . In brief, suitable satellites are chosen from all available satellites (those located within the visible area) and phases are calculated. Then the algorithm in *D* updates the phases for the chosen satellites to keep the power gain constantly ideal for ground nodes. Once any satellite becomes unavailable, we return to the beginning and the above process repeats.

V. Simulations

Simulations are conducted to verify the effectiveness of the proposed algorithm. The settings are listed in Table I. In this section, if not specially mentioned, the power gain in each refers to the average power gain of all UEs, and the score is defined as (14.)

A. Factors Affecting Power Distribution

In this section, we examine how satellite locations and the transmit phase affect the power distribution on the ground. The satellite number is 4.

First, the influence of satellite locations is examined. The transmit phases are set to be 0 on all satellites. The locations of satellites are varied. Then we show the influence of transmit phases. The satellite locations are settled and the phases are randomly chosen within $[-\pi, \pi]$. The comparisons are shown in Fig. 8. It can be seen that both satellite locations and transmit phases largely affect power distribution, thus making it feasible to adjust power distribution according to the distribution of UEs on the ground. Comparing the effect of changing satellite locations and phases, it can be seen that the former changes the distribution pattern of the ground power gain. The locations of spots are changed. While for phases, the distribution is not seriously altered, but still the central positions of spots shift.

B. GA-based Distributed Beamforming

The GA algorithm selects the most suitable satellite and their transmit phases. 20 experiments are conducted. For each experiment, we set 10 satellites within the available area and 7 ground UE on the ground, both randomly. For each experiment, 4 satellites are selected and transmit phases are calculated according to Algorithm I.

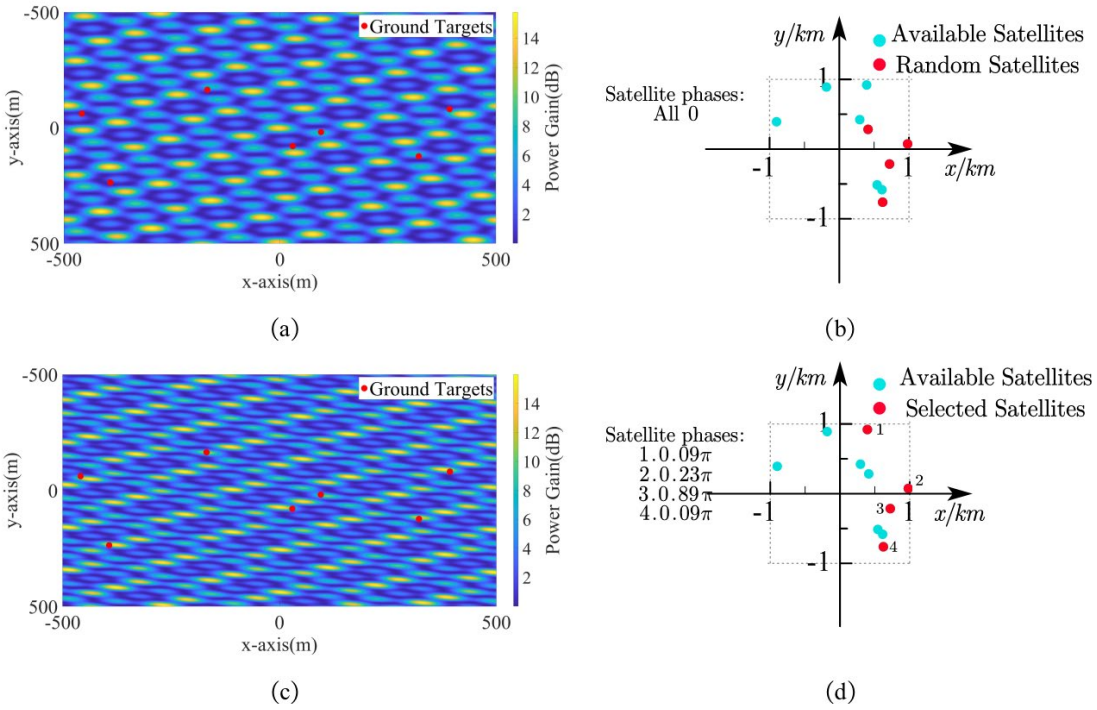

Fig. 4 Results of GA optimization.

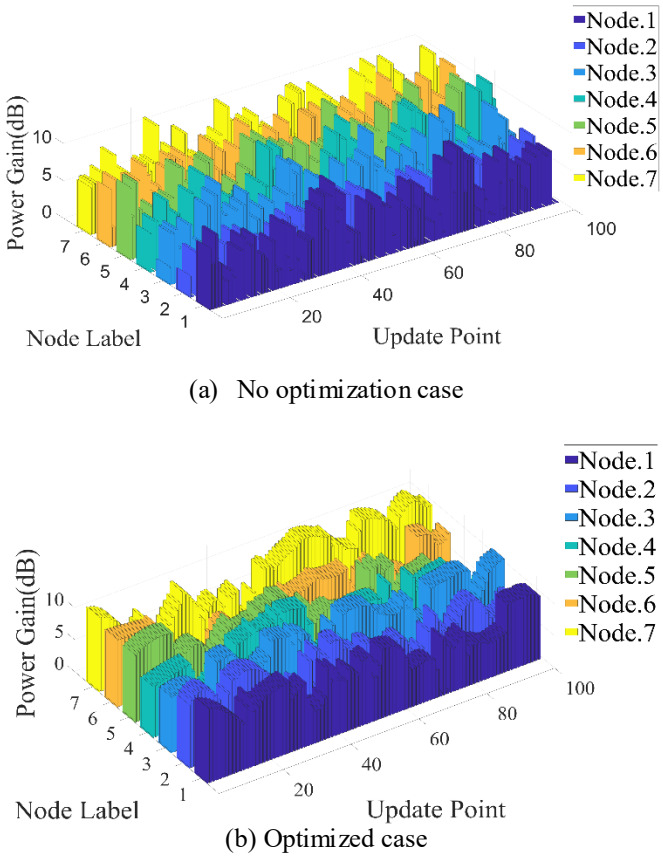

Fig. 11 The power gain of nodes on every update point. (a) the case without optimization and (b) the optimized case.

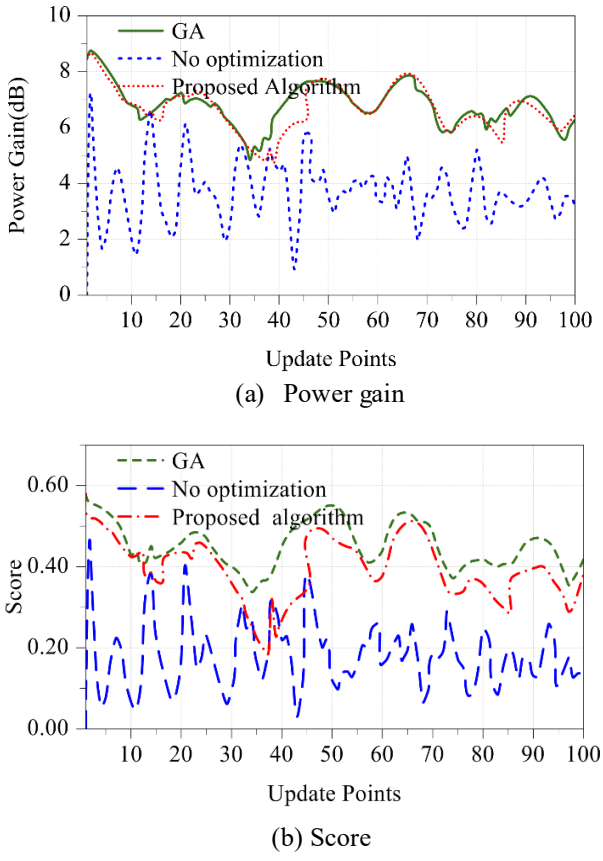

Fig. 12 Power gain and score on each update point. (a) The power gain and (b) the score.

The statistical results of 20 experiments are shown in Fig. 9. 2 different results are shown. Score refers to g defined as(14), power gain is calculated as(11). The baseline case refers to that satellite are randomly chosen and phases are set to 0, meaning there's no optimization. The comparison of the proposed algorithm to the baseline shows that our algorithm has ideal

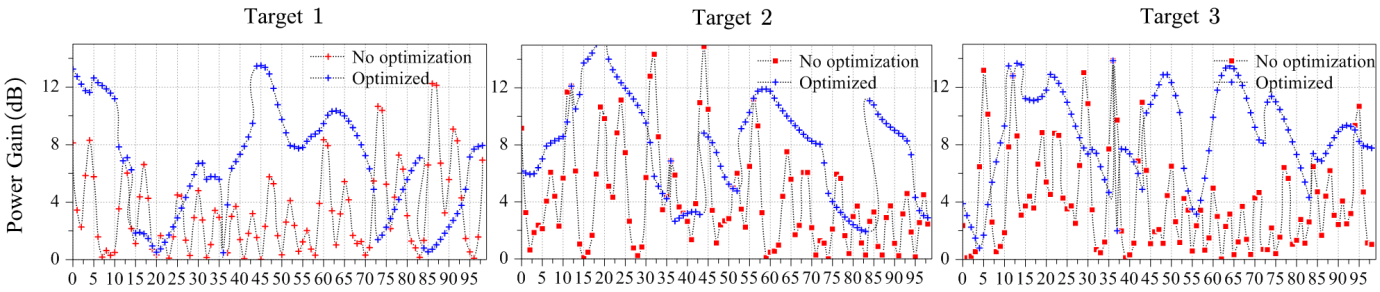

Fig. 14 Power gain of different ground targets.

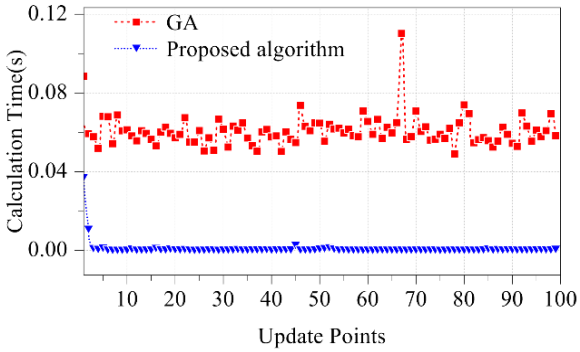

Fig. 13 Calculation time comparison.

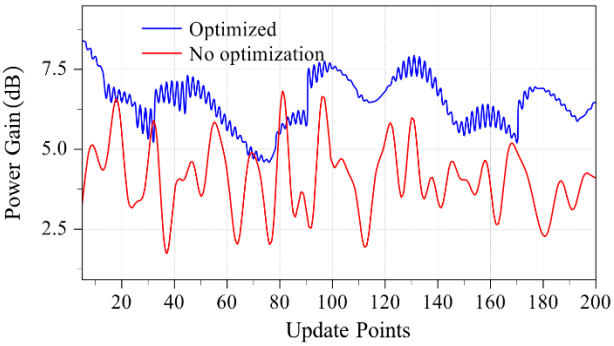

Fig. 15 Power gain condition between and on each update point.

performance in most cases, no matter the distribution of satellites and ground UEs. For example, in experiment 6, the power gain increases up to 7dB, and the score of power condition for ground UEs, defined as (14), raised from 0.13 to 0.71 (maximum 1). Note that score is a better judgment of the power gain improvement of all UEs, however, the average power gain is more intuitive and easier to understand. Thus both of them are shown for better demonstration of the proposed algorithm.

We pick one experiment (Label 6) and show detailed results. To better illustrate the effect of our algorithm, the power gain figures on the ground are shown ((a) and (c)). The satellite selection and according phase are also presented ((b) and (d)). (a) and (b) are the original cases with random satellite selection and no phase adjustment. (c) and (d) are the optimized case. The comparison between the ground power gain before and after optimization demonstrates the effectiveness of Algorithm I. Also, it can be seen that the power distribution figure is changed. The UEs (red points) are more widely covered by bright regions with higher gains.

C. Distributed Beamforming with Moving Satellites

We further demonstrate the effectiveness of the proposed algorithm for moving satellites (Algorithm II). Fig 11 shows the power gain of all the nodes on every update point. We compare two cases. (a) is the case without optimization, i.e. as the satellite moves, the phases stay the same, while (b) is the optimized case where phases are calculated and updated according to Algorithm II throughout the whole process. It can be seen that the proposed algorithm significantly increases the overall power gain.

To better demonstrate the effect of dynamic phase adjustment, the condition of the power gain as well as the score are shown in Fig 12. For the GA case, at each update point, the phases are calculated by the GA algorithm as Algorithm I, which has a longer calculation time but is more likely to achieve a better solution. The comparison shows that our algorithm has a great improvement in both power gain and the score compared to the no-optimization case. The power gain is increased up to 4dB, and the score is increased around 0.5. Also, our algorithm approaches the GA algorithm even though it has a much shorter calculation time.

We also demonstrate that the proposed algorithm has a short enough calculation time so that it can be used for moving satellites and adjust phases according to changing satellite locations. The calculation time of GA and our algorithm of each update point is compared in Fig 13. It is obvious that the proposed algorithm has a much shorter calculation time. Specifically, its average calculation time is only about 1.5% of GAs.

To show detailed results of our algorithm, we show power gain of different UEs separately in Fig 13. Three UEs are picked out and the power gains before and after optimization are shown. It is illustrated that the power gain improvement is ideal from the perspective of individual UE. This global optimization leads to that on some points, the power gain of some UEs may not be ideal. However, the overall power gain is always optimal.

A potential concern for our algorithm is that between each update point, the calculated phases may not be suitable for consistently moving satellites. To examine this, we settle the update point and test the ground power gain and score twice as frequently as the update calculation. By doing this, the condition of ground power gain between update points is

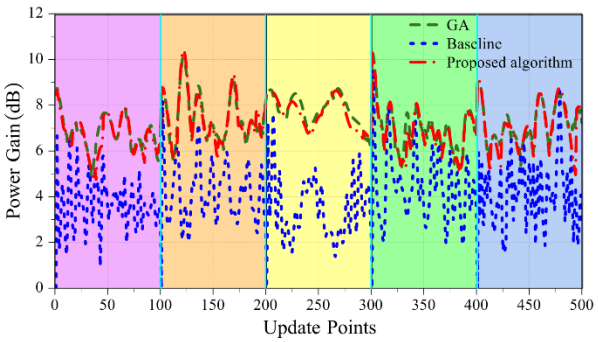

Fig. 16 Power gain throughout the process of satellite reselections.

checked. In Fig 14, we double the sampling the ground power gain detection to see the power gain condition between update points. Although on once every two update points the phases are not optimized for the temporal satellite locations, the optimized case exhibits an overall advantages over the no-optimization case. Notice that on some points, the optimized case is no better than the no-optimization case, because satellite moves to locations that are seriously unsuitable for calculated phases on the previous point. These conditions are rare and thus can be accepted.

The satellite reselection process is also simulated. We conduct 5 rounds of selection (Satellites are re-selected for 4 times.) and show the average power gain and score throughout the whole process, as Fig 16. The point of satellite reselection is marked out with blue lines. In each color region, four satellites are chosen and the phases are updated as satellites move.

The results demonstrate that our algorithm can provide consistent power gain improvement regardless of the satellite distribution and movement. Compared to the baseline (No optimization), the proposed algorithm can provide a constant power gain increase of around 3dB. Also, its performance approaches GAs, despite that the calculation time is much shorter.

V. Conclusion

This work proposes a distributed beamforming scheme for satellites that can simultaneously increase the receiving power gain of multiple ground UEs. The overlapping phenomenon of electromagnetic waves is discussed and the factors influencing the resulting power gain distribution on the ground are analyzed. We design an algorithm that selects appropriate satellites from some available ones and calculates the transmit phases on satellites. This algorithm ensures that UEs on the ground receive ideal power gains. Results show that the algorithm can increase up to 9dB of power gain. This work also considers satellite motion and proposes a fast algorithm that adjusts the phases according to the changing locations of satellites. Results demonstrate the effectiveness and show that the calculation time is short enough for dynamic update. Finally, a satellite re-selection scheme is designed to ensure a consistent power gain improvement when satellites are no longer available. Results demonstrate that the design can provide a power gain increase of around 3 dB throughout the process.

References

[1] Del Portillo I, Cameron B G, Crawley E F. A technical comparison of three low earth orbit satellite constellation systems to provide global broadband[J]. Acta astronautica, 2019, 159: 123-135.

[2] T. Darwish, G. K. Kurt, H. Yanikomeroglu, M. Bellemare and G. Lamontagne, "LEO Satellites in 5G and Beyond Networks: A Review From a Standardization Perspective," in *IEEE Access*, vol. 10, pp. 35040-35060, 2022, doi: 10.1109/ACCESS.2022.3162243

[3] S. Chen, Y.-C. Liang, S. Sun, S. Kang, W. Cheng, and M. Peng, "Vision, requirements, and technology trend of 6G: How to tackle the challenges of system coverage, capacity, user data-rate and movement speed," *IEEE Wireless Commun.*, vol. 27, no. 2, pp. 218–228, Apr. 2020, doi: 10.1109/MWC.001.1900333.

[4] D. Tuzi, T. Delamotte and A. Knopp, "Satellite Swarm-Based Antenna Arrays for 6G Direct-to-Cell Connectivity," in *IEEE Access*, vol. 11, pp. 36907-36928, 2023, doi: 10.1109/ACCESS.2023.3257102.

[5] Apple to Debut iPhone With Emergency Messaging Enabled by Globalstar Satellites. Accessed: Sep. 8, 2022. [Online]. Available:https://www.satellitetoday.com/telecom/2022/09/07/apple-to debut iPhone-with-emergency-messaging-enabled-by-globalstar-satellites/

[6] (Sep. 2022). The First Phone maker to Add Satellite Texting to Its Devices is...Huawei. Accessed: Sep. 14, 2022.[Online]. Available:https://www.theverge.com/2022/9/6/23339717/huawei-mate-50-pro satellite-text-china-beidou

[7] Lynk Global, "Messaging from an orbital base station to cellular user equipment applications with message processing via a card operating system," U.S. Patent US20210360587A1, Nov. 18, 2021.

[8] L. You, K. -X. Li, J. Wang, X. Gao, X. -G. Xia and B. Ottersten, "Massive MIMO Transmission for LEO Satellite Communications," in *IEEE Journal on Selected Areas in Communications*, vol. 38, no. 8, pp. 1851-1865, Aug. 2020, doi: 10.1109/JSAC.2020.3000803.

[9] P. Wang, J. Liu, C. Zhou, B. Yin and W. Wang, "Dual-Band Dual-Circularly Polarized Fabry-Pérot Cavity MIMO Antenna Using CMM-Based Polarization Converter and MMA for Vehicular Satellite Communications," in *IEEE Transactions on Vehicular Technology*, vol. 72, no. 7, pp. 8844-8856, July 2023, doi: 10.1109/TVT.2023.3245203.

[10] M. Alsenwi, E. Lagunas and S. Chatzinotas, "Robust Beamforming for Massive MIMO LEO Satellite Communications: A Risk-Aware Learning Framework," in *IEEE Transactions on Vehicular Technology*, vol. 73, no. 5, pp. 6560-6571, May 2024, doi: 10.1109/TVT.2023.3338065.

[11] You L, Qiang X, Li K X, et al. Hybrid analog/digital precoding for downlink massive MIMO LEO satellite communications[J]. *IEEE Transactions on Wireless Communications*, 2022, 21(8): 5962-5976.

[12] El-Din M S H S, Shams S I, Allam A, et al. SIGW based MIMO antenna for satellite down-link applications[J]. *IEEE Access*, 2022, 10: 35965-35976.

[13] C. Li, H. Zhu, J. Tang, J. Hu and G. Li, "User Grouping in Multiuser Satellite MIMO Downlink With Fairness Consideration," in *IEEE Wireless Communications Letters*, vol. 11, no. 8, pp. 1575-1579, Aug. 2022, doi: 10.1109/LWC.2022.3165807.

[14] R. Mudumbai, D. R. Brown Iii, U. Madhow and H. V. Poor, "Distributed transmit beamforming: challenges and recent progress," in *IEEE Communications Magazine*, vol. 47, no. 2, pp. 102-110, February 2009, doi: 10.1109/MCOM.2009.4785387.

[15] R. Mudumbai, G. Barriac and U. Madhow, "On the Feasibility of Distributed Beamforming in Wireless Networks," in *IEEE Transactions on Wireless Communications*, vol. 6, no. 5, pp. 1754-1763, May 2007, doi: 10.1109/TWC.2007.360377.

[16] M. Wentz and K. R. Chowdhury, "Intra-Network Synchronization and Retrodirective Distributed Transmit Beamforming With UAVs," in *IEEE Transactions on Vehicular Technology*, vol. 73, no. 2, pp. 2017-2031, Feb. 2024, doi: 10.1109/TVT.2023.3311733.

[17] N. Xie, K. Xu and J. Chen, "Exploiting Cumulative Positive Feedback Information for One-Bit Feedback Synchronization Algorithm," in *IEEE Transactions on Vehicular Technology*, vol. 67, no. 7, pp. 5821-5830, July 2018, doi: 10.1109/TVT.2018.2798809.

[18] Dagres I, Polydoros A, Moustakas A. Performance analysis of distributed beamforming in wireless networks: The effect of synchronization and Doppler spread[C]//MILCOM 2021-2021 *IEEE Military Communications Conference* (MILCOM). IEEE, 2021: 957-962.
[19] Ouassal H, Yan M, Nanzer J A. Decentralized frequency alignment for collaborative beamforming in distributed phased arrays[J]. *IEEE Transactions on Wireless Communications*, 2021, 20(10): 6269-6281.
[20] J. Kong, F. T. Dagefu and B. M. Sadler, "Distributed Beamforming in the Presence of Adversaries," in *IEEE Transactions on Vehicular Technology*, vol. 69, no. 9, pp. 9682-9696, Sept. 2020, doi: 10.1109/TVT.2020.3001532.
[21] D. Jang, H. -L. Song, Y. -C. Ko and H. J. Kim, "Distributed Beam Tracking for Vehicular Communications via UAV-Assisted Cellular Network," in *IEEE Transactions on Vehicular Technology*, vol. 72, no. 1, pp. 589-600, Jan. 2023, doi: 10.1109/TVT.2022.3202369.
[22] Hanna S, Cabric D. Distributed transmit beamforming: Design and demonstration from the lab to UAVs[J]. *IEEE Transactions on Wireless Communications*, 2022, 22(2): 778-792.
[23] H. Jung, I. -H. Lee and J. Joung, "Security Energy Efficiency Analysis of Analog Collaborative Beamforming With Stochastic Virtual Antenna Array of UAV Swarm," in *IEEE Transactions on Vehicular Technology*, vol. 71, no. 8, pp. 8381-8397, Aug. 2022, doi: 10.1109/TVT.2022.3171313.
[24] Alemdar K, Varshney D, Mohanti S, et al. RFClock: Timing, phase and frequency synchronization for distributed wireless networks[C]//Proceedings of the 27th Annual International Conference on Mobile Computing and Networking. 2021: 15-27.
[25] Sun G, Li J, Wang A, et al. Collaborative beamforming for UAV networks exploiting swarm intelligence[J]. *IEEE Wireless Communications*, 2022, 29(4): 10-17.
[26] Fan X, Ding H, Zhang Y, et al. Distributed beamforming based wireless power transfer: Analysis and realization[J]. Tsinghua Science and Technology, 2020, 25(6): 758-775.
[27] Shen S, Kim J, Song C, et al. Wireless power transfer with distributed antennas: System design, prototype, and experiments[J]. *IEEE Transactions on Industrial Electronics*, 2020, 68(11): 10868-10878.
[28] Shen S, Kim J, Song C, et al. Wireless power transfer with distributed antennas: System design, prototype, and experiments[J]. *IEEE Transactions on Industrial Electronics*, 2020, 68(11): 10868-10878.
[29] Shen S, Clerckx B. Joint waveform and beamforming optimization for MIMO wireless power transfer[J]. *IEEE Transactions on Communications*, 2021, 69(8): 5441-5455.
[30] Xu Z, Chen G, Fernandez R, et al. Enhancement of Direct LEO Satellite-to-Smartphone Communications by Distributed Beamforming[J]. *IEEE Transactions on Vehicular Technology*, 2024.
[31] E. Juan, M. Lauridsen, J. Wigard and P. Mogensen, "Location-Based Handover Triggering for Low-Earth Orbit Satellite Networks," 2022 IEEE 95th Vehicular Technology Conference: (VTC2022-Spring), Helsinki, Finland, 2022, pp. 1-6, doi: 10.1109/VTC2022-Spring54318.2022.9860992.
[32] 5G; NR; User Equipment (UE) Radio Transmission and Reception; Part 1: Range 1 Standalone (3GPP TS 38.101-1 Version 17.6.0 Release 17), ETSI TS 138 101-1 V17.6.0, 3GPP, Sophia Antipolis, France, Jun. 2022.
[33] C. E. Fossa, R. A. Raines, G. H. Gunsch and M. A. Temple, "An overview of the IRIDIUM (R) low Earth orbit (LEO) satellite system," Proceedings of the IEEE 1998 National Aerospace and Electronics Conference. NAECON 1998. Celebrating 50 Years (Cat. No.98CH36185), Dayton, OH, USA, 1998, pp. 152-159, doi: 10.1109/NAECON.1998.710110
[34] Byrd, R.H., R.B. Schnabel, and G.A. Shultz, "Approximate Solution of the Trust Region Problem by Minimization over Two-Dimensional Subspaces," *Mathematical Programming*, Vol. 40, pp 247–263, 1988.

Qianyi Ouyang was born in China, in 2002. He received the B.S. degree in electronic engineering in 2024, and is currently pursuing the Ph.D. degree in computer science with Fudan University, Shanghai, China.

His research interests include wideband beamforming, array signal processing, and distributed beamforming.

Zhishu Qu (Member, IEEE) was born in China, in 1993. She received the B.S. and M.S. degrees in electromagnetic field and microwave technology from the University of Electronic Science and Technology of China (UESTC), Chengdu, China, in 2016 and 2019, respectively, and the Ph.D. degree in electronic engineering and computer science from the Queen Mary University of London (QMUL), London, U.K., in 2023. She is currently a Post-Doctoral Researcher at the School of Computer Science and the Director of the Intelligent Networking and Computing Research Centre, Fudan University, China. Her research interests include satellite communications, phased arrays, and beamforming.

Yue Gao (Fellow, IEEE) received the Ph.D. degree from the Queen Mary University of London (QMUL), U.K., in 2007. He is currently a Professor at the School of Computer Science and the Director of the Intelligent Networking and Computing Research Centre, Fudan University, China. He worked as a Lecturer, a Senior Lecturer, a Reader, and the Chair Professor at QMUL and the University of Surrey, respectively. His research interests include smart antennas, sparse signal processing, and cognitive networks for mobile and satellite systems. He has published over 200 peer-reviewed journal and conference papers and had over 6400 citations. He is a member of the Board of Governors. He was also elected as an Engineering and Physical Sciences Research Council fellow in 2017. He was a co-recipient of the EU Horizon Prize Award on collaborative spectrum sharing in 2016. He is a Distinguished Speaker of the IEEE Vehicular Technology Society (VTS). He is the Vice-Chair of the IEEE ComSoc Wireless Communication Technical Committee and the past Chair of the IEEE ComSoc Technical Committee on Cognitive Networks. He has been the Symposia Chair, the Track Chair, and other roles in the organising committee of several IEEE ComSoC, VTS, and other conferences. He has been an Editor of several IEEE transactions and journals.